Table 2 Relation between p53 expression and *TP53* gene status in gastric cancer

	TP53 gene status		*P* value
	Wild (n = 73)	Mutation (n = 17) (%)	
p53 expression			
Null ($n = 13$)	7 (9.6)	6 (35.3)	<0.0001
Scattered ($n = 45$)	45 (61.6)	0 (0)	
Aberrant ($n = 32$)	21 (28.8)	11 (64.7)	

Table 3 Relation between mortalin and p53 expression in gastric cancer

	Mortalin expression Negative ($n = 45$)	Positive ($n = 137$) (%)	*P* value
p53 expression			
Negative ($n = 92$)	35 (77.8)	57 (41.6)	<0.0001
Positive ($n = 90$)	10 (22.2)	80 (58.4)	

tumor suppression, its relationship with prognosis in cancer is controversial. Even large studies of *TP53* gene in colorectal cancer have not been able to establish the relationship between *TP53* gene mutation and prognosis [27, 28].

Mortalin is a member of the heat-non-inducible heat shock protein 70 family [29]. It is expressed under stressful conditions. Mortalin binds to and disrupts the function of p53 by inhibiting its entry into the nuclei [10, 11]. It seems reasonable for cancer cells to express mortalin to protect them against stressful conditions, avoid tumor suppressor p53 function, and prevent apoptosis.

In gastric cancer clinical samples, mortalin-positive and aberrant p53 tumors had more malignant features and poorer prognosis compared with mortalin-negative or aberrant p53 negative tumors. Mortalin and aberrant p53 expression had a significant relationship, and tumor cells that were positive for mortalin also expressed aberrant p53. Aberrant p53 accumulated in the nuclei, which could have resulted in more malignant features. It is known that mortalin is expressed under stressful conditions [4–6]. In cancer cells with aberrant p53, the normal function of p53 is disrupted, and these cancer cells do not undergo apoptosis under stressful conditions. In these cancer cells, a stressed condition might influence mortalin expression by gene copy number gains or epigenetically function (e.g., hypo-methylation). This alteration of mortalin expression may prevent apoptosis.

The most notable finding in this study is that mortalin expression resulted in malignant features in gastric cancer

Table 4 Mortalin expression and clinicopathological factors in gastric cancer patients with scattered p53 expression

Factors	Mortalin expression		*P*-value
	Negative ($n = 27$)	Positive ($n = 48$) (%)	
Age (meant ± SD)	59.9 ± 11.9	64.8 ± 12.7	0.04
Gender			
Male	17 (63.0)	30 (62.5)	0.96
Female	10 (37.0)	18 (37.5)	
Differentiation			
Differentiated	11 (40.7)	16 (33.3)	0.52
Undifferentiated	16 (59.3)	32 (66.7)	
Vascular involvement			
V0	17 (63.0)	31 (64.6)	0.81
V1	8 (29.6)	13 (27.1)	
V2	2 (6.7)	3 (6.3)	
V3	0 (0)	1 (2.0)	
Lymphatic involvement			
Ly0	10 (37.0)	17 (35.4)	0.81
Ly1	5 (18.6)	10 (20.8)	
Ly2	6 (22.2)	14 (29.2)	
Ly3	6 (22.2)	7 (14 6)	
Depth of invasion			
M, SM	9 (33.3)	5 (10.4)	0.017**
MP, SS, SE, SI	18 (66.7)	43 (89.6)	
Lymph node metastasis			
Negative	14 (51.9)	16 (33.3)	0.11
Positive	13 (48.1)	32 (66.7)	
Stage			
I + II	14 (51.9)	21 (43.8)	0.49
III + IV	13 (48.1)	27 (56.2)	

M mucosa, *SM* submucosa, *MP* muscularis propria, *SS* subserosa, *SE* penetration of serosa, *SI* invasion of adjacent structures

** $P < 0.05$

with "scattered" p53 staining (Table 4; Fig. 4). This is suggested by the fact that mortalin expression was an independent prognostic factor in gastric cancer with "scattered" p53 staining (Table 5). In this study, we evaluated the significance of p53 immunohistochemistry staining in gastric cancer. By classifying the p53 staining pattern in three groups, we found that the "scattered" staining pattern of p53 reflected wild-type *TP53* gene. This result was consistent with a previous report on colorectal cancer done by Kaserer et al. [17]. They reported that this scattered staining type in colorectal cancer cells represents a functionally active non-mutated p53 gene. We might therefore be able to distinguish normal p53 function by immunohistochemistry staining of p53. "Scattered" type reflects normal p53 function.

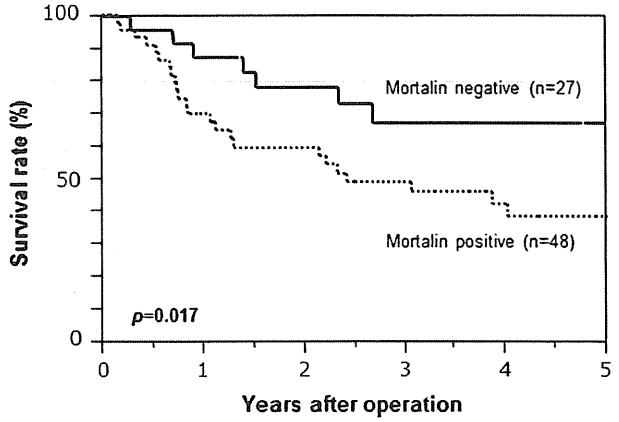

Fig. 4 Cumulative survival curve for gastric cancer patients with scattered p53 expression. Tumors with mortalin-positive expression had poor prognosis ($n = 75$, $P = 0.017$)

Table 5 Cox regression analysis for gastric cancer patients with scattered p53 expression

Explanatory variable (observed value)	*P* value	Relative risk (95 % confidence interval)
Vascular involvement (none vs. present)	0.41	2.83 (1.94–4.21)
Lymphatic involvement (none vs. present)	0.01*	11.3 (9.88–13.82)
Lymph node metastasis (none vs. present)	0.21	1.56 (1.25–3.08)
Differentiation (differentiated vs. undifferentiated)	0.004*	8.22 (5.98–8.58)
Mortalin (negative vs. positive)	0.013*	6.08 (5.0–7.97)

* Statistically significant

From this study, we found that mortalin is crucial for malignant features, even in gastric cancer with normal p53. Our results suggest that mortalin expression is an independent prognostic factor in such gastric cancer. Mortalin is known to bind to p53 and to prevent the entry of p53 into the nucleus and disrupt its normal function. In gastric cancer with expression of normal p53, mortalin might disrupt normal p53 function as a tumor suppressor and benefit cancer cells. To treat gastric cancer that has mortalin expression, a drug that avoids mortalin and p53 binding could be useful. MKT-077 is a rhodacyanine dye analog that preferentially accumulates in tumor cells [30]. It has been reported that its selective toxicity to tumor cells is mediated by binding to mortalin and reactivation of p53 function [31]. Although a phase I trial of MKT-077 with chemoresistant solid tumors failed because of renal toxicity [32], there remains a possibility for using the drug in mortalin-expressing tumors. Deocaris et al. [33] have reported that in tumor cells with elevated mortalin expression, low doses of MKT-077 are sufficient to induce senescence and might prevent renal toxicity. In deciding on the usage of MKT-077, investigation of mortalin expression by immunohistochemical staining might be a useful tool. MKT-077 may be effective in gastric cancer with normal p53 and mortalin-positive expression.

Our results show that mortalin expression is a prognostic marker in gastric cancer, especially in tumors with normal p53 function. When choosing mortalin as a target molecule, p53 expression is a selective marker, which may result in effective therapy.

Acknowledgments We thank Ms. Y. Kubota for her preparation of the immunohistochemistry samples.

References

1. Wadhwa R, Kaul SC, Ikawa Y, Sugimoto Y. Identification of a novel member of mouse hsp70 family. Its association with cellular mortal phenotype. J Biol Chem. 1993;268:6615–21.
2. Kaul SC, Duncan E, Sugihara T, Reddel RR, Mitsui Y, Wadhwa R. Structurally and functionally distinct mouse hsp70 family members Mot-1 and Mot-2 proteins are encoded by two alleles. DNA Res. 2000;7:229–31.
3. Kaul SC, Duncan EL, Englezou A, Takano S, Reddel RR, Mitsui Y, Wadhwa R. Malignant transformation of NIH3T3 cells by overexpression of mot-2 protein. Oncogene. 1998;17:907–11.
4. Liu Y, Liu W, Song XD, Zuo J. Effect of GRP75/mthsp70/PBP74/mortalin overexpression on intracellular ATP level, mitochondrial membrane potential and ROS accumulation following glucose deprivation in PC12 cells. Mol Cell Biochem. 2005;268:45–51.
5. Merrick BA, Walker VR, He C, Patterson RM, Selkirk JK. Induction of novel Grp75 isoforms by 2-deoxyglucose in human and murine fibroblasts. Cancer Lett. 1997;119:185–90.
6. Sadekova S, Lehnert S, Chow TY. Induction of PBP74/mortalin/Grp75, a member of the hsp70 family, by low doses of ionizing radiation: a possible role in induced radioresistance. Int J Radiat Biol. 1997;72:653–60.
7. Mizukoshi E, Suzuki M, Loupatov A, Uruno T, Hayashi H, Misono T, Kaul SC, Wadhwa R, Imamura T. Fibroblast growth factor-1 interacts with the glucose-regulated protein GRP75/mortalin. Biochem J. 1999;343(Pt 2):461–6.
8. Takano S, Wadhwa R, Mitsui Y, Kaul SC. Identification and characterization of molecular interactions between glucose-regulated proteins (GRPs) mortalin/GRP75/peptide-binding protein 74 (PBP74) and GRP94. Biochem J. 2001;357:393–8.
9. Wadhwa R, Yaguchi T, Hasan MK, Taira K, Kaul SC. Mortalin–MPD (mevalonate pyrophosphate decarboxylase) interactions and their role in control of cellular proliferation. Biochem Biophys Res Commun. 2003;302:735–42.
10. Wadhwa R, Takano S, Robert M, Yoshida A, Nomura H, Reddel RR, Mitsui Y, Kaul SC. Inactivation of tumor suppressor p53 by mot-2, a hsp70 family member. J Biol Chem. 1998;273:29586–91.
11. Wadhwa R, Yaguchi T, Hasan MK, Mitsui Y, Reddel RR, Kaul SC. Hsp70 family member, mot-2/mthsp70/GRP75, binds to the cytoplasmic sequestration domain of the p53 protein. Exp Cell Res. 2002;274:246–53.
12. Wadhwa R, Takano S, Kaur K, Deocaris CC, Pereira-Smith OM, Reddel RR, Kaul SC. Upregulation of mortalin/mthsp70/Grp75

contributes to human carcinogenesis. Int J Cancer. 2006;118: 2973–80.
13. Wadhwa R, Takano S, Taira K, Kaul SC. Reduction in mortalin level by its antisense expression causes senescence-like growth arrest in human immortalized cells. J Gene Med. 2004;6:439–44.
14. Dundas SR, Lawrie LC, Rooney PH, Murray GI. Mortalin is over-expressed by colorectal adenocarcinomas and correlates with poor survival. J Pathol. 2005;205:74–81.
15. Aikou T, Hokita S, Natsugoe S. Japanese classification of gastric carcinoma (the 13th edition, June 1999): points to be revised. Nippon Rinsho. 2001;59(Suppl 4):159–65.
16. Elledge RM, Clark GM, Fuqua SA, Yu YY, Allred DC. p53 protein accumulation detected by five different antibodies: relationship to prognosis and heat shock protein 70 in breast cancer. Cancer Res. 1994;54:3752–7.
17. Kaserer K, Schmaus J, Bethge U, Migschitz B, Fasching S, Walch A, Herbst F, Teleky B, Wrba F. Staining patterns of p53 immunohistochemistry and their biological significance in colorectal cancer. J Pathol. 2000;190:450–6.
18. Rodrigues NR, Rowan A, Smith ME, Kerr IB, Bodmer WF, Gannon JV, Lane DP. p53 mutations in colorectal cancer. Proc Natl Acad Sci USA. 1990;87:7555–9.
19. Sumiyoshi Y, Kakeji Y, Egashira A, Mizokami K, Orita H, Maehara Y. Overexpression of hypoxia-inducible factor 1alpha and p53 is a marker for an unfavorable prognosis in gastric cancer. Clin Cancer Res. 2006;12:5112–7.
20. el-Deiry WS, Kern SE, Pietenpol JA, Kinzler KW, Vogelstein B. Definition of a consensus binding site for p53. Nat Genet. 1992; 1:45–9.
21. Miyashita T, Reed JC. Tumor suppressor p53 is a direct transcriptional activator of the human bax gene. Cell. 1995;80:293–9.
22. Nakano K, Vousden KH. PUMA, a novel proapoptotic gene, is induced by p53. Mol Cell. 2001;7:683–94.
23. Oda E, Ohki R, Murasawa H, Nemoto J, Shibue T, Yamashita T, Tokino T, Taniguchi T, Tanaka N. Noxa, a BH3-only member of the Bcl-2 family and candidate mediator of p53-induced apoptosis. Science. 2000;288:1053–8.
24. Momand J, Zambetti GP, Olson DC, George D, Levine AJ. The mdm-2 oncogene product forms a complex with the p53 protein and inhibits p53-mediated transactivation. Cell. 1992;69: 1237–45.
25. Beroud C, Soussi T. The UMD-p53 database: new mutations and analysis tools. Hum Mutat. 2003;21:176–81.
26. Hussain SP, Harris CC. Molecular epidemiology of human cancer: contribution of mutation spectra studies of tumor suppressor genes. Cancer Res. 1998;58:4023–37.
27. Munro AJ, Lain S, Lane DP. P53 abnormalities and outcomes in colorectal cancer: a systematic review. Br J Cancer. 2005;92: 434–44.
28. Russo A, Bazan V, Iacopetta B, Kerr D, Soussi T, Gebbia N. The TP53 colorectal cancer international collaborative study on the prognostic and predictive significance of p53 mutation: influence of tumor site, type of mutation, and adjuvant treatment. J Clin Oncol. 2005;23:7518–28.
29. Kaul SC, Deocaris CC, Wadhwa R. Three faces of mortalin: a housekeeper, guardian and killer. Exp Gerontol. 2007;42:263–74.
30. Koya K, Li Y, Wang H, Ukai T, Tatsuta N, Kawakami M, Shishido T, Chen LB. MKT-077, a novel rhodacyanine dye in clinical trials, exhibits anticarcinoma activity in preclinical studies based on selective mitochondrial accumulation. Cancer Res. 1996;56:538–43.
31. Wadhwa R, Sugihara T, Yoshida A, Nomura H, Reddel RR, Simpson R, Maruta H, Kaul SC. Selective toxicity of MKT-077 to cancer cells is mediated by its binding to the hsp70 family protein mot-2 and reactivation of p53 function. Cancer Res. 2000;60:6818–21.
32. Propper DJ, Braybrooke JP, Taylor DJ, Lodi R, Styles P, Cramer JA, Collins WC, Levitt NC, Talbot DC, Ganesan TS, Harris AL. Phase I trial of the selective mitochondrial toxin MKT077 in chemo-resistant solid tumours. Ann Oncol. 1999;10:923–7.
33. Deocaris CC, Widodo N, Shrestha BG, Kaur K, Ohtaka M, Yamasaki K, Kaul SC, Wadhwa R. Mortalin sensitizes human cancer cells to MKT-077-induced senescence. Cancer Lett. 2007;252:259–69.

Surg Today
DOI 10.1007/s00595-013-0581-x

ORIGINAL ARTICLE

Contribution of Aurora-A and -B expression to DNA aneuploidy in gastric cancers

Kenichi Honma · Ryota Nakanishi · Tomonori Nakanoko · Koji Ando · Hiroshi Saeki · Eiji Oki · Makoto Iimori · Hiroyuki Kitao · Yoshihiro Kakeji · Yoshihiko Maehara

Received: 15 August 2012 / Accepted: 7 January 2013

Abstract
Purpose DNA aneuploidy, which is characterized by cells containing an abnormal number of chromosomes, is closely associated with carcinogenesis and malignant progression. Aneuploidy occurs during cell division when the chromosomes do not separate properly. Aurora kinases (Aurora-A, -B, and -C) contribute to accurate cell division, and are candidate molecular targets for mitosis-specific anticancer drugs.
Methods We determined the expression of Aurora-A and -B in 110 gastric cancer specimens by performing an immunohistochemical analysis. We also determined the DNA content, *TP53* gene mutations, and microsatellite instability in the same samples.
Results We found the nuclear expression of Aurora-A and -B to increase in tumor tissue in comparison to that in normal epithelial tissue. A high Aurora-B expression significantly correlated with aneuploidy and *TP53* mutations, but not with microsatellite instability. In contrast, the Aurora-A expression did not correlate with either aneuploidy or microsatellite instability. In addition, the expression of Aurora-A or -B was not significantly associated with the clinical outcomes or prognosis.
Conclusions Our results suggest that an overexpression of Aurora-B, but not of Aurora-A, might contribute to DNA aneuploidy in gastric cancers by promoting chromosomal instability.

Keywords Aurora-B · Aneuploidy · Gastric cancer

Introduction

DNA aneuploidy, defined as cells containing an abnormal number of chromosomes, is a hallmark of cancer. Aneuploidy is closely associated with chromosomal instability pathway (CIN) [1–3], one of two major pathways of genomic destabilization in gastric carcinogenesis [4]. CIN is characterized by whole or fractional chromosomal gains and losses [5, 6]. The second pathway, namely the microsatellite instability pathway (MIN), is associated with a near-diploid karyotype and a relatively low frequency of allelic losses. MIN is caused by mismatch repair deficiency and leads to alterations in genomic repeat sequences such as microsatellite sequences [7]. These alterations in microsatellite sequences are known as microsatellite instability (MSI) [7, 8].

It has been reported that CIN contributes to carcinogenesis and may predict cancer progression and poor prognosis [9]. Although many studies have focused on aneuploidy and CIN, the cellular and molecular mechanisms of aneuploidy and CIN are not yet fully understood. Aneuploidy occurs during cell division and represents a state when the chromosomes do not separate properly [9, 10]. When improper kinetochore-spindle attachments are detected by the cell, then the spindle checkpoint is activated, which prevents mitotic progression by activating several checkpoint agents including Bub1, BubR1, Mps1, Mad1, and Mad2 [11]. Several studies have shown that defects in these genes are likely to cause CIN [12, 13].

K. Honma · R. Nakanishi · T. Nakanoko · K. Ando · H. Saeki · E. Oki · Y. Kakeji · Y. Maehara
Department of Surgery and Science, Graduate School of Medical Sciences, Kyushu University, Fukuoka, Japan

R. Nakanishi · M. Iimori · H. Kitao (✉)
Department of Molecular Oncology, Graduate School of Medical Sciences, Kyushu University, 3-1-1 Maidashi, Higashi-ku, Fukuoka 812-8582, Japan
e-mail: hkitao@surg2.med.kyushu-u.ac.jp

Published online: 10 April 2013

Aurora kinases represent a family of serine/threonine kinases crucial for cell cycle control. Mammalian genomes contain at least three genes encoding Aurora kinases: Aurora-A, -B, and -C. Of these, Aurora-A and -B have received the greatest attention because defects in these kinases may lead to severe mitotic abnormalities. Aurora-A and -B regulate cell preparation to enter mitosis, the formation of the mitotic spindle, sister chromatid separation, chromosome-spindle attachments, and cytokinesis with several co-activators [14]. Aurora-A is mainly involved in the centrosome function and spindle assembly [15]. The dysfunction of Aurora-A leads to abnormal spindle morphology and defects in chromosome segregation [16]. Aurora-B forms the chromosomal passenger complex with inner centromere protein, Borealin/Dasra, and Survivin. These subunits coordinate the localization of Aurora-B to the central spindle [17]. Aurora-B is thought to be involved in cytokinesis because the inhibition of the Aurora-B activity causes disrupts cytokinesis [18]. It has been reported that Aurora kinases are overexpressed in human cancer tissues, including gastric cancers [19, 20]. Moreover, the overexpression of Aurora-B causes multinuclearity and increased ploidy in human cancer cells [21]. Therefore, the aim of our present study was to examine the effects of Aurora kinase expression on genomic instability in gastric cancers.

Methods

Patients and specimens

We analyzed 110 consecutive patients with gastric cancer who underwent surgical resection at the Department of Surgery and Science, Kyushu University Hospital, between 1994 and 2006. The characteristics and follow-up times of these patients are summarized in Table 1. The histological diagnosis was based on the World Health Organization criteria [22]. Pathologic staging was performed according to the tumor-node-metastasis classification system as revised in 2002 [23]. The median follow-up time of these patients was 21.2 months (range 1–113 months). Written informed consent was obtained from all patients. The institutional review board of our university approved this study.

Immunohistochemistry

An immunohistochemical analysis was carried out on formalin-fixed, paraffin-embedded tissue sections. Four-micrometer sections were deparaffinized and heat-induced epitope retrieval was performed at 121 °C for 15 min in

Table 1 Relationship among clinicopathologic factors and DNA aneuploidy

Characteristics	All patients ($N = 110$)	Patients with tumors exhibiting DNA euploidy ($N = 42$)	Patients with tumors exhibiting DNA aneuploidy ($N = 68$)	P value
Age, years	64.3 ± 12.4	61.6 ± 14.2	66.0 ± 10.9	0.09
Sex, no. (%)				
Male	74 (67)	27 (64)	47 (69)	0.60
Female	36 (33)	15 (36)	21 (31)	
Tumor grade, no. (%)				
Well differentiated	26 (24)	7 (17)	19 (29)	–
Moderately differentiated	23 (21)	4 (10)	19 (29)	
Poorly differentiated	48 (44)	26 (62)	22 (33)	
Others	13 (12)	5 (12)	8 (12)	
Depth of invasion, no. (%)				
T1, T2	25 (22)	8 (19)	17 (25)	0.46
T3, T4	85 (78)	34 (81)	51 (75)	
Infiltration, no. (%)[a]				
α	9 (9)	2 (5)	7 (11)	0.06
β or γ	90 (91)	36 (95)	54 (89)	
Lymphatic invasion, no. (%)[b]				
–	34 (31)	6 (14)	28 (42)	0.0018
+	75 (69)	36 (86)	39 (58)	
Vein invasion, no. (%)[c]				
–	66 (61)	29 (69)	37 (55)	0.15
+	43 (39)	13 (31)	30 (44)	
Lymph node metastasis, no. (%)				
–	25 (23)	10 (24)	15 (22)	0.83
+	85 (77)	32 (76)	53 (78)	
Metastasis, no. (%)				
–	106 (96)	41 (98)	65 (96)	0.57
+	4 (4)	1 (2)	3 (4)	
Hepatic metastasis, no. (%)				
–	105 (95)	40 (95)	65 (96)	0.93
+	5 (5)	2 (5)	3 (4)	
MSI, no. (%)				
MSI-S or L	98 (89)	34 (81)	64 (94)	0.034
MSI-H	12 (11)	8 (19)	4 (6)	
Stage of tumor, no. (%)				
I	21 (19)	9 (21)	12 (18)	–
II	19 (17)	6 (14)	13 (19)	
III	26 (24)	7 (17)	19 (28)	
IV	44 (40)	20 (48)	24 (35)	
TP53 mutation, no. (%)				
–	59 (54)	23 (55)	36 (53)	0.11
+	20 (18)	4 (10)	16 (24)	

Table 1 continued

Characteristics	All patients ($N = 110$)	Patients with tumors exhibiting DNA euploidy ($N = 42$)	Patients with tumors exhibiting DNA aneuploidy ($N = 68$)	P value
Status, no. (%)				
Dead	53 (48)	23 (55)	30 (44)	–
Alive	57 (52)	19 (45)	38 (56)	
Follow up (months) (median)	21.2	19.6	22.7	–

MSI-S microsatellite stable, *MSI-L* low frequency of microsatellite instability, *MSI-H* high frequency of microsatellite instability

[a] 11 missing data

[b] 1 missing data

[c] 1 missing data

0.1 M citrate buffer (pH 6.0) for Aurora-A or antigen retrieval buffer (pH 9.0) (Abcam, Cambridge, UK) for Aurora-B. The slides were incubated with rabbit polyclonal antibodies against Aurora-A (NOVUS Biologicals, Littleton, CO) or Aurora-B (Cell Signaling Technology, Beverly, MA) overnight at 4 °C. The sections were then washed and treated with Envision Plus anti-rabbit secondary antibodies (DAKO, Glostup, Denmark). Staining for Aurora-A and -B was completed using the streptavidin–biotin–peroxidase complex method with diaminobenzidine as a chromogen. We evaluated the nuclear staining of Aurora-A and -B (Fig. 1). The immunoreactivity score (IRS) for Aurora-A was determined as the multiplication of the values for the grade of intensity (0 = no staining, 1 = weak, 2 = moderate, 3 = strong) and the number of positive cells (1 = 0–10, 2 = 11–50, 3 = 51–80, 4 = >80 %). The Aurora-A expression was classified as high when the IRS was ≥3 (median value) and as low when the IRS was ≤2. Aurora-B staining was evaluated as previously described [24]. Immunohistochemical expression was evaluated in a semi-quantitative manner in 1,000 tumor cells. The patients were classified into two groups based on Aurora-B expression: high (Aurora-B-positive cells detected in >10 % of tumor cells; median value) or low (Aurora-B-positive cells detected in <10 % of tumor cells). Appropriate positive and negative controls were included in each run of immunohistochemistry. The expression levels of Aurora-A and -B were determined by four researchers, including two clinicopathologists, who were all blinded to the patients' clinical characteristics.

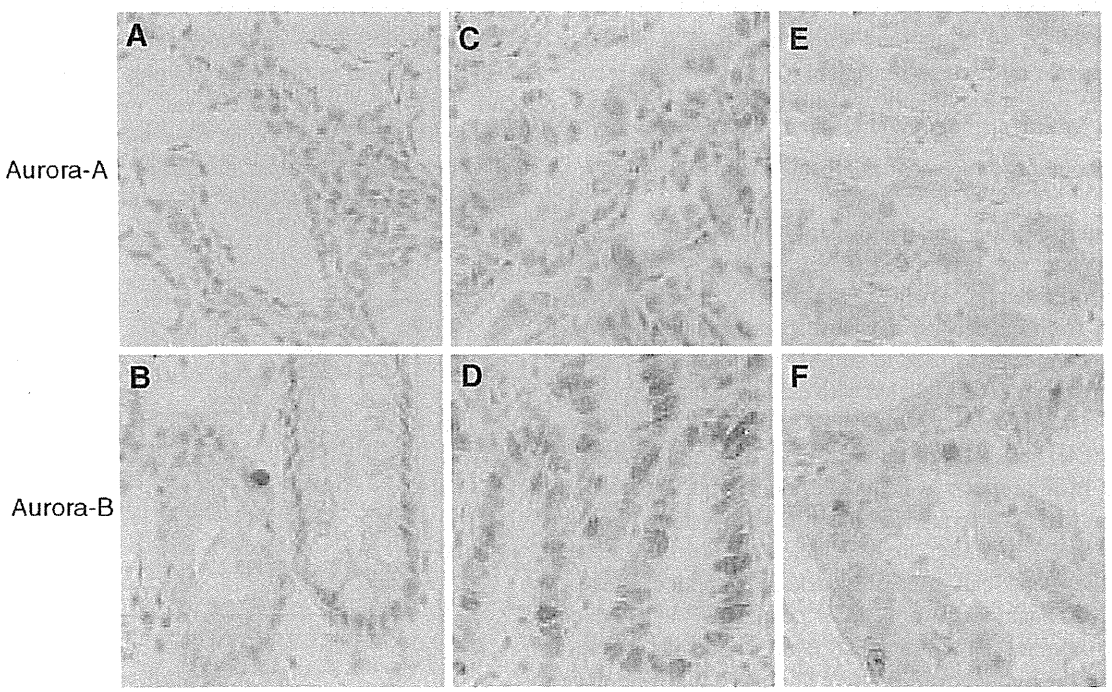

Fig. 1 Localization of Aurora-A and -B proteins in human gastric tissue determined by immunohistochemistry. **a**, **b** Normal epithelium. **c–f** Gastric cancer tissue. Aurora-A was weakly expressed in normal epithelial tissue (**a**) but was frequently expressed in gastric cancer tissue (**c**). Some gastric cancer specimens showed low nuclear expression of Aurora-A (**e**). Aurora-B was rarely observed in normal epithelial tissue (**b**) but was frequently expressed in gastric cancer tissue (**d**). Some gastric cancer specimens showed a low nuclear expression of Aurora-B (**f**). (**a–f**, magnification ×400)

Analysis of DNA ploidy

Nuclear DNA content was measured by laser scanning cytometry (CompuCyte, Westwood, MA), as previously described [25, 26]. The same paraffin-embedded blocks that were used for immunohistochemical staining were used for this analysis. A DNA content histogram was generated and DNA ploidy was determined. The DNA index (DI) was calculated according to previously published criteria [27, 28]. For each sample, the nuclei were observed after each scan to exclude debris and attached nuclei from the analysis. The DI of G0/G1-phase lymphocytes or fibroblasts was used as a reference value, and allocated a DI of 1.0. Tumors with a DI < 1.2 were defined as diploid. Tumors with a DI > 1.2 or multi-indexed samples were defined as aneuploid. Aneuploidy was confirmed by single nucleotide polymorphism comparative genomic hybridization (SNP–CGH) arrays [29, 30].

TP53 gene mutation analysis

The *TP53* gene exons 5–9, including the exon–intron junctions, were amplified by polymerase chain reaction (PCR) using primers for *P53* (Nippon Gene, Tokyo, Japan) and Ex Taq DNA polymerase (Takara Bio, Tokyo, Japan). The PCR products were purified and used as templates for cycle-sequencing reactions with the Big Dye Terminator Cycle Sequencing Kit version 1 (Applied Biosystems, Foster City, CA). Mutations found in the PCR products were verified by reverse sequencing and then were reconfirmed in two independently amplified PCR products.

High-resolution fluorescent microsatellite analysis

The microsatellite analysis using fluorescence-labeled primers and an automated DNA sequencer has been described in detail elsewhere [31]. Briefly, genomic DNA isolated from cancerous and corresponding noncancerous tissue specimens was used to amplify microsatellite loci by PCR using primer sets labeled with a fluorescent compound, either ROX (6-carboxy-x-rhodamine) or HEX (6-carboxy-20,40,70,4,7,-hexachloro-fluorescein). The fluorescently labeled PCR products were mixed, denatured, and loaded onto an ABI 310 sequencer (Applied Biosystems, Foster City, CA) for fragment analysis. The data were processed using the GeneScan software package (Applied Biosystems). MSI positive was defined as a change in the length of a microsatellite PCR fragment from cancerous tissues. Based on the frequency of positive findings of five reference markers, MSI was classified as high (MSI-H) when detected in at least two markers, low (MSI-L) when detected in one marker, or microsatellite stable (MSS) when no positive MSIs were detected in any of the loci.

Statistical analysis

The relationships among clinicopathologic factors and Aurora-A and -B expression were analyzed using χ^2 tests and logistic regression analysis. Survival curves between the subgroups divided by DNA aneuploidy or the expression levels of Aurora-A or Aurora-B were plotted using the Kaplan–Meier method, and significant differences among the subgroups were compared using the log-rank test. The Cox proportional hazards multivariate regression analysis with the forward stepwise procedure was used to identify factors independently associated with prognosis. Values of $P < 0.05$ were considered to be statistically significant.

Results

Genomic instability in patients with gastric cancers

We investigated the characteristics of aneuploidy in 110 clinical samples of gastric cancer. DNA content was measured by laser scanning cytometry in these samples. Tumors displaying aneuploidy were observed in 68 out of 110 patients (62 %; Table 1). There was no correlation between aneuploidy and clinicopathological factors except for lymphatic invasion. Furthermore, aneuploidy was not associated with the prognosis (Fig. 2). To evaluate the relationship between two carcinogenic pathways, namely CIN and MIN, *TP53* gene mutations and MSI status were also determined in the same samples by direct sequencing and high-resolution fluorescent microsatellite analysis (Table 1). *TP53* gene exons were analyzed in 79 patients, of which 20 (25 %) had mutations. The MSI status was analyzed in 110 patients, of which 12 (11 %) were

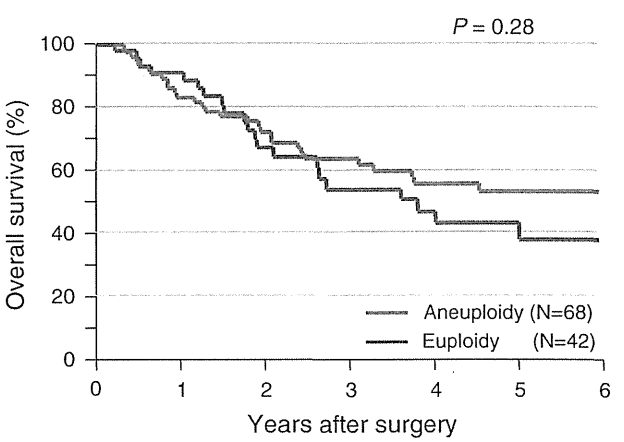

Fig. 2 Kaplan–Meier estimates of the 5-year overall survival (OS) according to DNA ploidy. There was no significant difference in the OS between patients with aneuploid tumors and patients with diploid tumors

considered to be MSI-positive. Patients with tumors exhibiting aneuploidy more frequently had *TP53* mutations, although this was not statistically significant ($P = 0.11$). Aneuploidy was inversely correlated with MSI-H ($P = 0.034$).

Protein expression of Aurora-A and -B in gastric cancers

We determined the protein expression of Aurora-A and -B by immunohistochemistry in 110 clinical samples of gastric cancer (Fig. 1). The expression levels of both Aurora-A and -B were significantly greater in tumor tissue than in normal epithelial tissue (Fig. 1a–d). To evaluate the clinical significance of the expression levels of Aurora-A and -B, we classified the patients into two groups according to the median immunohistological reactivity of Aurora-A or -B (Fig. 1c–f). Accordingly, nuclear Aurora-A was found to be high in 55 patients (50 %). As shown in Table 2, the protein expression level of Aurora-A was significantly associated with lymphatic invasion ($P = 0.032$) and metastasis (except for hepatic or peritoneal metastasis) ($P = 0.017$). In contrast, the protein expression level of Aurora-B was significantly associated with age ($P = 0.0047$), venous invasion ($P = 0.020$), and peritoneal metastasis ($P = 0.0063$) (Table 2). The expression levels of Aurora-A and -B were not significantly associated with the prognosis ($P = 0.67$ and 0.44, respectively; Fig. 3).

Aurora kinase expression and aneuploidy in gastric cancers

We analyzed the relationship between DNA ploidy and the expression levels of Aurora-A and -B to determine whether these Aurora kinases were associated with aneuploidy in gastric cancers. Interestingly, as shown in Table 3, we found no correlation between the Aurora-A expression and DNA ploidy ($P = 0.24$), *TP53* mutations ($P = 0.55$) or the MSI status ($P = 1.00$). We also evaluated the cytoplasmic expression of Aurora-A, but there was no correlation between this pattern of Aurora-A expression and these clinicopathologic factors (data not shown). In contrast, aneuploidy was significantly more frequent among tumors with a high Aurora-B expression ($P = 0.023$, Table 3). The Aurora-B expression also significantly correlated with *TP53* gene mutations ($P = 0.010$), but not with MSI ($P = 0.63$, Table 3).

Aurora kinase expression and prognosis in gastric cancers

The prognoses for patients with a low or high expression of Aurora-A were equal ($P = 0.95$, data not shown). The patients with *TP53* gene mutations and a high Aurora-B expression tended to have worse prognoses, although this finding was not statistically significant ($P = 0.35$, data not shown). When either of the kinases were overexpressed, the patients with *TP53* gene mutations had similar outcomes to the patients without *TP53* gene mutations ($P = 0.95$, data not shown).

Discussion

We conducted this study to examine the contribution of Aurora kinases to aneuploidy in gastric cancers. We assessed the relationship between the expression levels of Aurora-A and -B with DNA aneuploidy, *TP53* gene mutations, and MSI status, as well as with the clinicopathological factors and the prognosis in patients with gastric cancers. Our results indicate that a high expression of Aurora-B, but not of Aurora-A, significantly correlated with DNA aneuploidy. We also found the expression levels of Aurora-A and -B to be significantly higher in tumor tissue than in normal epithelial tissue. The Aurora-A expression correlated with lymphatic invasion and metastasis and Aurora-B with venous invasion and peritoneal metastasis; however, neither the Aurora-A nor -B expression correlated with prognosis (Table 2; Fig. 3).

Previous studies have led to the identification of two major pathways of genomic destabilization in gastric carcinogenesis, CIN and MIN [2, 6, 7]. Several studies have also documented the clinical significance of DNA aneuploidy in gastric cancers [32, 33]. Gastric carcinoma with aneuploidy is characterized by a high proliferative activity and a high metastatic or invasive potential, thus resulting in a worse prognosis compared with diploid tumors [32]. In our study, we analyzed samples from 110 patients with gastric cancer, 68 (62 %) of which exhibited DNA aneuploidy. This frequency was consistent with that described in a previous study [32], but DNA aneuploidy was not associated with either malignant characteristics or a poor prognosis in our study (Table 1; Fig. 2), which is not consistent with the previous study. We consider that this discrepancy may have been caused by non-standardized tumor staging and the selected therapeutic strategies. A more homogeneous patient population may be needed to better understand the long-term influence of aneuploidy on survival.

Tumor suppressor genes, such as *TP53*, *RB*, and *APC*, are believed to be critically involved in the suppression of carcinogenesis through CIN. Mutations in the *TP53* gene contribute to CIN and aneuploidy [34]. We confirmed that *TP53* gene mutations occurred more frequently in tumors with aneuploidy than in tumors with diploidy, but this finding was not statistically significant ($P = 0.11$;

Table 2 Relationship among the clinicopathologic factors and Aurora kinases expression

Characteristics	Aurora-A		*P* value	Aurora-B		*P* value
	Low expression ($N = 55$)	High expression ($N = 55$)		Low expression ($N = 53$)	High expression ($N = 57$)	
Age, years	64.1 ± 12.4	64.5 ± 12.4	0.70	60.3 ± 14.0	67.9 ± 9.3	0.0047
Sex, no. (%)						
Male	37 (67)	37 (67)	1.00	32 (60)	42 (74)	0.14
Female	18 (33)	18 (33)		21 (40)	15 (26)	
Tumor grade, no. (%)						
Well differentiated	16 (30)	10 (19)	–	12 (23)	14 (25)	–
Moderately differentiated	8 (15)	15 (28)		6 (11)	17 (30)	
Poorly differentiated	24 (43)	24 (43)		29 (55)	19 (33)	
Others	7 (13)	6 (11)		6 (11)	7 (12)	
Depth of invasion, no. (%)						
T1, T2	11 (20)	14 (25)	0.49	11 (21)	14 (25)	0.63
T3, T4	44 (80)	41 (75)		42 (79)	43 (75)	
Infiltration, no. (%)[a]						
α	7 (14)	2 (4)	0.23	2 (4)	7 (14)	0.08
β or γ	44 (86)	46 (96)		47 (96)	43 (86)	
Lymphatic invasion, no. (%)[b]						
–	22 (41)	12 (22)	0.032	15 (28)	19 (34)	0.53
+	32 (59)	43 (78)		38 (72)	37 (66)	
Vein invasion, no. (%)[c]						
–	32 (59)	34 (62)	0.78	38 (72)	28 (50)	0.020
+	22 (41)	21 (38)		15 (28)	28 (50)	
Lymph node metastasis, no. (%)						
–	12 (22)	13 (24)	0.82	13 (25)	12 (21)	0.66
+	43 (78)	42 (76)		40 (75)	45 (79)	
Metastasis, no. (%)						
–	55 (100)	51 (93)	0.017	52 (98)	54 (95)	0.33
+	0 (0)	4 (7)		1 (2)	3 (5)	
Hepatic metastasis, no. (%)						
–	53 (96)	52 (95)	0.65	52 (98)	53 (93)	0.18
+	2 (4)	3 (5)		1 (2)	4 (7)	
Peritoneal metastasis, no. (%)						
–	48 (87)	48 (87)	1.00	41 (77)	55 (96)	0.0063
+	7 (13)	7 (13)		12 (23)	2 (4)	
Stage of tumor, no. (%)						
I	8 (15)	13 (24)	–	10 (19)	11 (19)	–
II	12 (22)	7 (13)		8 (15)	11 (19)	
III	16 (29)	10 (18)		9 (17)	17 (30)	
IV	19 (35)	25 (45)		26 (49)	18 (32)	

[a] 11 missing data

[b] 1 missing data

[c] 1 missing data

Table 1). When either Aurora-A or -B was overexpressed, the patients with *TP53* gene mutations had similar outcomes to the patients without *TP53* gene mutations ($P = 0.95$, data not shown). It has been reported that *TP53* loss of function mutations are associated with overt multipolar mitoses in esophageal cancer cell lines [35]. Larger

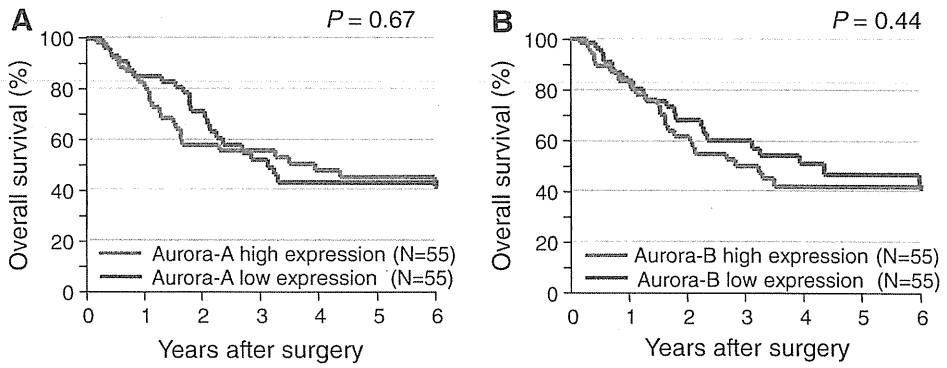

Fig. 3 Kaplan–Meier estimates of the 5-year overall survival (OS) according to the expression levels of Aurora-A (**a**) and Aurora-B (**b**)

Table 3 Relationship among the Aurora kinases expression levels and DNA aneuploidy

Characteristics	Aurora-A		*P* value	Aurora-B		*P* value
	Low expression ($N = 55$)	High expression ($N = 55$)		Low expression ($N = 53$)	High expression ($N = 57$)	
DNA ploidy, no. (%)						
Euploidy	24 (44)	18 (33)	0.24	26 (49)	16 (28)	0.023
Aneuploidy	31 (56)	37 (67)		27 (51)	41 (72)	
TP53 mutation, no. (%)[a]						
–	34 (77)	25 (71)	0.55	34 (87)	25 (63)	0.010
+	10 (23)	10 (29)		5 (13)	15 (37)	
MSI, no. (%)						
MSI-S or L	49 (89)	49 (89)	1.00	48 (91)	50 (88)	0.63
MSI-H	6 (11)	6 (11)		5 (9)	7 (12)	

[a] 31 missing data

trials with more comprehensive investigation into patient background may be needed to address this discrepancy.

Aurora-A is localized at the spindles and their poles, and it plays an important role in the centrosome function, mitotic entry, and spindle assembly [15]. Aurora-A is often overexpressed in human cancers, and its overexpression in a human cancer cell line has been reported to block cytokinesis [36]. The overexpression of Aurora-A has also been reported to lead to aneuploidy and a malignant phenotype in various types of cancer [37–39]. Although *AURKA* gene overexpression was reported to be associated with aneuploidy in gastric cancers, no studies have so far reported a relationship between Aurora-A protein expression and aneuploidy in gastric cancers [40]. In our study, Aurora-A overexpression was not correlated with aneuploidy or *TP53* gene mutations. Our results therefore suggest that Aurora-A overexpression is not associated with aneuploidy or CIN in gastric cancers.

Aurora-B plays an important role in the correction of incorrect kinetochore-microtubule attachments and progression of cytokinesis [17, 18]. Similar to *AURKA*, *AURKB*-transfected cells have been reported to have an unstable chromosome number and displayed an aggressive phenotype in vivo [21, 41, 42]. However, in studies of surgical specimens, the relationship between Aurora-B expression and DNA ploidy has been controversial [43, 44]. In our study, Aurora-B overexpression was correlated with aneuploidy and *TP53* mutations. It has been reported that Aurora-B overexpression contributes to the development of cancer in concert with CIN and aneuploidy [21]. Our data support the idea that Aurora-B overexpression may contribute to the induction of the CIN phenotype in gastric cancers. Several inhibitors of Aurora kinases have been clinically evaluated as anticancer drugs [14]. Therefore, targeting Aurora B using these inhibitors may represent an effective strategy to kill tumors with CIN in patients with gastric cancers.

Acknowledgments We are grateful to Ms. Yoko Kubota for her valuable technical assistance.

Conflict of interest Hiroyuki Kitao and other co-authors have no conflict of interest.

References

1. Thompson SL, Compton DA. Examining the link between chromosomal instability and aneuploidy in human cells. J Cell Biol. 2008;180:665–72.

2. Thompson SL, Bakhoum SF, Compton DA. Mechanisms of chromosomal instability. Curr Biol. 2010;20:R285–95.
3. Schvartzman JM, Sotillo R, Benezra R. Mitotic chromosomal instability and cancer: mouse modelling of the human disease. Nat Rev Cancer. 2010;10:102–15.
4. Lengauer C, Kinzler KW, Vogelstein B. Genetic instabilities in human cancers. Nature. 1998;396:643–9.
5. Yamashita K, Sakuramoto S, Watanabe M. Genomic and epigenetic profiles of gastric cancer: potential diagnostic and therapeutic applications. Surg Today. 2011;41:24–38.
6. Pellman D. Cell biology: aneuploidy and cancer. Nature. 2007; 446:38–9.
7. Boland CR, Goel A. Microsatellite instability in colorectal cancer. Gastroenterology. 2010;138(2073–2087):e2073.
8. Tokunaga E, Oki E, Oda S, et al. Frequency of microsatellite instability in breast cancer determined by high-resolution fluorescent microsatellite analysis. Oncology. 2000;59:44–9.
9. Albertson DG, Collins C, McCormick F, Gray JW. Chromosome aberrations in solid tumors. Nat Genet. 2003;34:369–76.
10. Sen S. Aneuploidy and cancer. Curr Opin Oncol. 2000;12:82–8.
11. Sjoblom T, Jones S, Wood LD, et al. The consensus coding sequences of human breast and colorectal cancers. Science. 2006;314:268–74.
12. Ando K, Kakeji Y, Kitao H, et al. High expression of BUBR1 is one of the factors for inducing DNA aneuploidy and progression in gastric cancer. Cancer Sci. 2010;101:639–45.
13. Cahill DP, Lengauer C, Yu J, et al. Mutations of mitotic checkpoint genes in human cancers. Nature. 1998;392:300–3.
14. Lens SM, Voest EE, Medema RH. Shared and separate functions of polo-like kinases and aurora kinases in cancer. Nat Rev Cancer. 2010;10:825–41.
15. Holland AJ, Cleveland DW. Boveri revisited: chromosomal instability, aneuploidy, and tumorigenesis. Nat Rev Mol Cell Biol. 2009;10:478–87.
16. Barr AR, Gergely F. Aurora-A: the maker and breaker of spindle poles. J Cell Sci. 2007;120:2987–96.
17. Vader G, Medema RH, Lens SM. The chromosomal passenger complex: guiding Aurora-B through mitosis. J Cell Biol. 2006;173:833–7.
18. Ditchfield C, Johnson VL, Tighe A, et al. Aurora B couples chromosome alignment with anaphase by targeting BubR1, Mad2, and Cenp-E to kinetochores. J Cell Biol. 2003;161: 267–80.
19. Yuan B, Xu Y, Woo JH, et al. Increased expression of mitotic checkpoint genes in breast cancer cells with chromosomal instability. Clin Cancer Res. 2006;12:405–10.
20. Enjoji M, Iida S, Sugita H, et al. BubR1 and AURKB overexpression are associated with a favorable prognosis in gastric cancer. Mol Med Report. 2009;2:589–96.
21. Tatsuka M, Katayama H, Ota T, et al. Multinuclearity and increased ploidy caused by overexpression of the aurora- and Ipl1-like midbody-associated protein mitotic kinase in human cancer cells. Cancer Res. 1998;58:4811–6.
22. Jass JR SL. Histological typing of intestinal tumours. WHO International Histological Classification of Tumours No. 15. 2nd ed. Berlin: Springer. 1989.
23. Sobin LH WC, editors. TNM Classification of malignant tumours, 6th ed. New York: Wiley–Liss. 2002.
24. Chieffi P, Cozzolino L, Kisslinger A, et al. Aurora B expression directly correlates with prostate cancer malignancy and influence prostate cell proliferation. Prostate. 2006;66:326–33.
25. Kamada T, Sasaki K, Tsuji T, et al. Sample preparation from paraffin-embedded tissue specimens for laser scanning cytometric DNA analysis. Cytometry. 1997;27:290–4.
26. Sasaki K, Kurose A, Miura Y, et al. DNA ploidy analysis by laser scanning cytometry (LSC) in colorectal cancers and comparison with flow cytometry. Cytometry. 1996;23:106–9.
27. Furuya T, Uchiyama T, Murakami T, et al. Relationship between chromosomal instability and intratumoral regional DNA ploidy heterogeneity in primary gastric cancers. Clin Cancer Res. 2000;6:2815–20.
28. Hiddemann W, Schumann J, Andreef M, et al. Convention on nomenclature for DNA cytometry. Committee on nomenclature, society for analytical cytology. Cancer Genet Cytogenet. 1984;13:181–3.
29. Oki E, Hisamatsu Y, Ando K, et al. Clinical aspect and molecular mechanism of DNA aneuploidy in gastric cancers. J Gastroenterol. 2012;47:351–8.
30. Brenner BM, Rosenberg D. High-throughput SNP/CGH approaches for the analysis of genomic instability in colorectal cancer. Mutat Res. 2010;693:46–52.
31. Oda S, Oki E, Maehara Y, Sugimachi K. Precise assessment of microsatellite instability using high resolution fluorescent microsatellite analysis. Nucleic Acids Res. 1997;25:3415–20.
32. Baba H, Korenaga D, Kakeji Y, et al. DNA ploidy and its clinical implications in gastric cancer. Surgery. 2002;131:S63–70.
33. Doak SH. Aneuploidy in upper gastro-intestinal tract cancers—a potential prognostic marker? Mutat Res. 2008;651:93–104.
34. Duensing A, Duensing S. Guilt by association? p53 and the development of aneuploidy in cancer. Biochem Biophys Res Commun. 2005;331:694–700.
35. Fichter CD, Herz C, Munch C, et al. Occurrence of multipolar mitoses and association with Aurora-A/-B kinases and p53 mutations in aneuploid esophageal carcinoma cells. BMC Cell Biol. 2011;12:13.
36. Meraldi P, Honda R, Nigg EA. Aurora-A overexpression reveals tetraploidization as a major route to centrosome amplification in p53−/− cells. EMBO J. 2002;21:483–92.
37. Baba Y, Nosho K, Shima K, et al. Aurora-A expression is independently associated with chromosomal instability in colorectal cancer. Neoplasia. 2009;11:418–25.
38. Wang X, Zhou YX, Qiao W, et al. Overexpression of aurora kinase A in mouse mammary epithelium induces genetic instability preceding mammary tumor formation. Oncogene. 2006;25:7148–58.
39. Lassus H, Staff S, Leminen A, et al. Aurora-A overexpression and aneuploidy predict poor outcome in serous ovarian carcinoma. Gynecol Oncol. 2011;120:11–7.
40. Sakakura C, Hagiwara A, Yasuoka R, et al. Tumour-amplified kinase BTAK is amplified and overexpressed in gastric cancers with possible involvement in aneuploid formation. Br J Cancer. 2001;84:824–31.
41. Ota T, Suto S, Katayama H, et al. Increased mitotic phosphorylation of histone H3 attributable to AIM-1/Aurora-B overexpression contributes to chromosome number instability. Cancer Res. 2002;62:5168–77.
42. Chen YJ, Chen CM, Twu NF, et al. Overexpression of Aurora B is associated with poor prognosis in epithelial ovarian cancer patients. Virchows Arch. 2009;455:431–40.
43. Burum-Auensen E, DeAngelis PM, Schjolberg AR, et al. Reduced level of the spindle checkpoint protein BUB1B is associated with aneuploidy in colorectal cancers. Cell Prolif. 2008;41:645–59.
44. Kulkarni AA, Loddo M, Leo E, et al. DNA replication licensing factors and aurora kinases are linked to aneuploidy and clinical outcome in epithelial ovarian carcinoma. Clin Cancer Res. 2007;13:6153–61.

Published OnlineFirst January 14, 2014; DOI: 10.1158/1078-0432.CCR-13-1645

Human Cancer Biology

Clinical Cancer Research

LINE-1 Hypomethylation, DNA Copy Number Alterations, and *CDK6* Amplification in Esophageal Squamous Cell Carcinoma

Yoshifumi Baba[1], Masayuki Watanabe[1], Asuka Murata[1], Hironobu Shigaki[1], Keisuke Miyake[1], Takatsugu Ishimoto[1], Masaaki Iwatsuki[1], Shiro Iwagami[1], Naoya Yoshida[1], Eiji Oki[3], Kentaro Sakamaki[4], Mitsuyoshi Nakao[2], and Hideo Baba[1]

Abstract

Purpose: Global DNA hypomethylation plays a crucial role in genomic instability and carcinogenesis. DNA methylation of the long interspersed nucleotide element-1, L1 (LINE-1) repetitive element is a good indicator of the global DNA methylation level, and is attracting interest as a useful marker for predicting cancer prognosis. Our previous study using more than 200 esophageal squamous cell carcinoma (ESCC) specimens demonstrated the significant relationship between LINE-1 hypomethylation and poor prognosis. However, the mechanism by which LINE-1 hypomethylation affects aggressive tumor behavior has yet to be revealed.

Experimental Design: To examine the relationship between LINE-1 hypomethylation and DNA copy number variations, we investigated LINE-1–hypomethylated and LINE-1–hypermethylated ESCC tumors by comparative genomic hybridization array.

Results: LINE-1–hypomethylated tumors showed highly frequent genomic gains at various loci containing candidate oncogenes such as *CDK6*. LINE-1 methylation levels were significantly associated with *CDK6* mRNA and CDK6 protein expression levels in ESCC specimens. In our cohort of 129 patients with ESCC, cases with CDK6-positive expression experienced worse clinical outcome compared with those with CDK6-negative expression, supporting the oncogenic role of CDK6 in ESCC. In addition, we found that the prognostic impact of LINE-1 hypomethylation might be attenuated by CDK6 expression.

Conclusion: LINE-1 hypomethylation (i.e., global DNA hypomethylation) in ESCC might contribute to the acquisition of aggressive tumor behavior through genomic gains of oncogenes such as *CDK6*. *Clin Cancer Res; 20(5); 1114–24. ©2014 AACR.*

Introduction

Esophageal squamous cell carcinoma (ESCC), the major histologic type of esophageal cancer in East Asian countries, is one of the most aggressive malignant tumors (1). Despite remarkable advances in multimodal therapies, including surgery, chemotherapy, radiotherapy, and chemoradiotherapy, the prognosis of patients remains poor, even for those whose carcinomas have been completely resected (2–4). To develop innovative strategies for treating ESCC, especially those that are molecularly targeted (5), it is of particular importance to increase our understanding of the cellular and molecular basis of this disease. Importantly, epigenetic changes, including alterations in DNA methylation, are reversible, and can thus be targets for cancer therapy or chemoprevention (6–8).

DNA methylation alterations occurring in human cancers include global DNA hypomethylation and site-specific CpG island promoter hypermethylation (9). Global DNA hypomethylation seems to play a crucial role in genomic instability, leading to cancer development (10–12). Because long interspersed nucleotide element-1 (LINE-1; L1 retrotransposon) constitutes a substantial portion (approximately 17%) of the human genome, the level of LINE-1 methylation is regarded to be a surrogate marker of global DNA methylation (13). In many types of human neoplasms, LINE-1 methylation has been shown to be highly variable (14–16), and LINE-1 hypomethylation is strongly associated with a poor prognosis (17–22). In a previous study of 217 curatively resected ESCC specimens (23), we

Authors' Affiliations: [1]Department of Gastroenterological Surgery, Graduate School of Medical Sciences; [2]Department of Medical Cell Biology, Institute of Molecular Embryology and Genetics, Kumamoto University, Kumamoto; [3]Department of Surgery and Science, Graduate School of Medical Sciences, Kyushu University, Fukuoka; and [4]Department of Biostatistics and Epidemiology, Yokohama City University Medical Center, Yokohama, Japan

Note: Supplementary data for this article are available at Clinical Cancer Research Online (http://clincancerres.aacrjournals.org/).

Corresponding Author: Hideo Baba, Graduate School of Medical Sciences, Kumamoto University, 1-1-1 Honjo, Kumamoto City, Kumamoto 860-8556, Japan. Phone: 81-96-373-5213; Fax: 81-96-373-4378; E-mail: hdobaba@kumamoto-u.ac.jp

doi: 10.1158/1078-0432.CCR-13-1645

Published OnlineFirst January 14, 2014; DOI: 10.1158/1078-0432.CCR-13-1645

Translational Relevance

The level of long interspersed nucleotide element-1 (LINE-1) methylation is regarded to be a surrogate marker of global DNA methylation. We have previously demonstrated that LINE-1 hypomethylation in esophageal squamous cell carcinoma (ESCC) is associated with a shorter survival, thus suggesting that it has potential for use as a prognostic biomarker. However, the mechanism by which LINE-1 hypomethylation affects aggressive tumor behavior has yet to be revealed. In this study, comparative genomic hybridization array revealed that LINE-1–hypomethylated ESCC tumors presented highly frequent genomic gains at various loci containing *CDK6*. In addition, LINE-1 methylation levels were associated with CDK6 expression in ESCCs and that the prognostic impact of LINE-1 hypomethylation in patients with ESCC was attenuated by CDK6 expression. Collectively, these findings may suggest that global DNA hypomethylation in ESCC might contribute to the acquisition of aggressive tumor behavior through genomic gains of oncogenes such as *CDK6*.

demonstrated that LINE-1 hypomethylation is associated with a poor prognosis, suggesting that LINE-1 hypomethylation may be a biomarker that can be used to identify patients who will experience an inferior outcome. However, the mechanism by which LINE-1 hypomethylation (and thus global DNA hypomethylation) may confer a poor prognosis remains to be fully explored. Given the known relationship between genome-wide DNA hypomethylation and genomic instability (24–27), we hypothesized that global DNA hypomethylation might be an important influential factor for DNA copy number variations, leading to altered expression levels of oncogenes or tumor suppressor genes.

To test this hypothesis, we investigated LINE-1–hypomethylated and LINE-1–hypermethylated ESCC tumors using array-based comparative genomic hybridization (CGH array). LINE-1–hypomethylated tumors showed highly frequent genomic gains at various loci containing candidate oncogenes such as *CDK6*. Thus, we further examined the correlation between LINE-1 methylation levels, *CDK6* amplification, CDK6 protein and mRNA expression, and clinical outcome.

Materials and Methods

Study subjects

All samples used in this study were collected at Kumamoto University Hospital (Kumamoto, Japan) between April 2005 and December 2011. LINE-1 methylation levels were quantified in 40 ESCC tumors for which freshly frozen specimens were available. Total RNA was obtained from 20 ESCC tumors, matched with 15 macroscopically normal esophageal tissues from the same patients. To assess the prognostic impact of CDK6 expression, we performed immunohistochemical staining of 129 ESCC samples. No patient received any preoperative treatment (chemotherapy, radiation therapy, or chemoradiotherapy). All 129 patients underwent curative resection. Tumor staging was performed according to the American Joint Committee on Cancer Staging Manual (seventh edition; ref. 28). Patients were observed at 1- to 3-month intervals until death or until March 31, 2013, whichever came first. Disease-free survival was defined as the period following surgical cancer treatment during which the patient survived with no sign of cancer recurrence. Among the 129 patients, 48 experienced disease recurrence during the follow-up period. This current analysis represents a new analysis of CDK6 on the existing ESCC database that has been previously characterized for LINE-1 methylation and clinical outcome (23). We have not examined CDK6 expression in any of our previous studies. Written informed consent was obtained from each subject, and the study procedures were approved by the institutional review board.

Pyrosequencing to measure LINE-1 methylation

Genomic DNA was extracted from frozen esophageal cancer specimens using a QIAamp DNA Mini Kit (Qiagen) according to the manufacturer's protocol. Genomic DNA was modified with sodium bisulfite using an EpiTect Bisulfite kit (Qiagen). PCR and subsequent pyrosequencing for LINE-1 were performed as previously described by Ogino and colleagues, using the PyroMark Kit (Qiagen; ref. 14). This assay amplifies a region of LINE-1 element (position 305 to 331, accession no. X58075), which includes four CpG sites. Pyrosequencing reactions were performed using the PyroMark Q24 System (Qiagen). Bisulfite pyrosequencing consists of three steps; bisulfite conversion, PCR amplification, and pyrosequencing analysis. Unmethylated cytosine and methylated cytosine are differentiated by bisulfite treatment followed by PCR. In the pyrosequencing step, the cytosine:methylated cytosine ratio at each CpG site is measured as the ratio of thymine:cytosine. The cytosine content relative to the cytosine plus thymine content at each CpG site is expressed as a percentage. In this study, the average relative cytosine content at the four CpG sites was used as the overall LINE-1 methylation level in a given tumor. In published literature, we have validated our LINE-1 methylation pyrosequencing assay; we performed bisulfite conversion on five different DNA specimen aliquots and repeated PCR pyrosequencing five times using four macrodissected cancers. Bisulfite-to-bisulfite (between-bisulfite treatment) SDs ranged from 1.4 to 2.9 (median, 2.3), and run-to-run (between-PCR pyrosequencing run) SDs ranged from 0.6 to 3.3 (median, 1.2; ref. 29).

Immunohistochemical staining

Paraffin-embedded tumor sections were dewaxed in xylene and ethanol, and antigen–epitope retrieval was performed using a streamer autoclave at 120°C for 15 minutes in antigen retrieval solution (pH9, Histofine; Nichirei Biosciences Inc.) and then allowed to cool. Endogenous peroxidase activity was blocked using 3% hydrogen peroxide.

Published OnlineFirst January 14, 2014; DOI: 10.1158/1078-0432.CCR-13-1645

Primary antibodies against CDK6 (1:50 dilution; Santa Cruz Biotechnology Inc.) and cyclin D1 (1:50 dilution; Leica Biosystems Newcastle Ltd) were applied, and the slides were incubated at 4°C overnight. The secondary antibody used was a ready-for-use anti-mouse EnVision Peroxidase system (Dako Japan Inc.). The remaining procedure was performed using a Dako EnVision+ System (Dako Japan Inc). The stained slides were counterstained with hematoxylin and bluing reagent. One of the investigators, blinded to any other participant data, recorded nuclear CDK6 and cyclin D1 expression as absent, weak, moderate, or strong. In this study, tumors with weak to strong expression were defined as "positive," whereas tumors not expressing these proteins were defined as "negative." Among 129 ESCC tumors, 61 tumors (47%) and 52 tumors (40%) tested positive for CDK6 and cyclin D1, respectively.

Quantitative reverse transcription PCR

Total RNA extraction, cDNA synthesis, and quantitative reverse transcription PCR (qRT-PCR) were carried out as previously described (30, 31). Total cellular RNA was extracted using the RNeasy Mini Kit (Qiagen), and cDNA was synthesized with the SuperScript III Transcriptor First Strand cDNA Synthesis System for RT-PCR (Invitrogen) according to the manufacturers' instructions. qRT-PCR was carried out using a LightCycler 480 II instrument (Roche). To determine the differences in the gene expression levels between specimens, the $2-\Delta\Delta Ct$ method was used to measure the fold changes among the samples. To carry out qRT-PCR, primers were designed using the Universal Probe Library (Roche) following the manufacturer's recommendations. The primer sequences and probes used for real-time PCR were as follows: *CDK6*, 5- TGATCAACTAGGAAAAATCTTGGA-3′, 5-GTCGACCGGTGCAATCTT-3′, and universal probe #2; glyceraldehyde-3-phosphate dehydrogenase (*GAPDH*), 5-AGCCACATCGCTCAGACAC-3′, 5-GCCCAATACGACCAAATCC-3′, and universal probe #60.

Array CGH

Array CGH was carried out using the Agilent oligonucleotide array–based CGH microarray kit (SurePrint G3 Human CGH Microarray Kit 2 × 400 K; Agilent Technologies) according to the manufacturer's protocol. Commercial male human genomic DNA was used as the control DNA. Following hybridization, washing, and drying steps, the microarray slides were scanned at 3 μm resolution, using the G2505C microarray scanner (Agilent Technologies). Features were extracted from the scanned images using the Feature Extraction software (version 1.5.1.0; Agilent Technologies). The extracted features were analyzed using the Agilent Cytogenomics software (version 2.0.6.0; Agilent Technologies).

Cell lines

Human esophageal cancer cell lines (TE-1, TE-4, TE-6, TE-8, TE-9, TE-10, TE-11, TE-14, and TE-15) were obtained from the Institute of Development, Aging, and Cancer, Tohoku University (Sendai, Japan) and were cultured in a medium supplemented with 10% FBS in 5% CO_2 atmosphere at 37°C.

FISH

CDK6-specific FISH probe was prepared using two human Bacterial Artificial Chromosomes (BAC) DNA clones RP11-809H24 and RP11-1102K14 by labeling with Cy3. As a control, a centromeric region-specific FISH probe for chromosome 7 was prepared using RP11-90C3. The images were captured with the CW4000 FISH application program (Leica Microsystems Imaging Solution).

Statistical methods

For the statistical analyses, we used the JMP software (version 9; SAS Institute). For the survival analysis, the Kaplan–Meier method was used to assess the survival time distribution, and the log-rank test was used. We constructed a CDK6-adjusted Cox proportional hazard model to compute the HR according to the LINE-1 methylation status. Statistical differences were considered significant if P values were <0.05. All reported P values are two-sided.

Results

Pyrosequencing assay for LINE-1 methylation status using frozen ESCC tissues

We quantified the LINE-1 methylation levels of 40 fresh-frozen esophageal cancer tissues using a bisulfite PCR pyrosequencing assay, and obtained valid results in all 40 cases. Representative pyrograms for LINE-1 methylation levels are shown in Fig. 1A. LINE-1 methylation levels in ESCC fresh-frozen tissues were distributed widely and approximately normally. The distribution was as follows: mean, 51.0; median, 52.6; SD, 14.8; range, 24.4–79.7; interquartile range, 38.6–62.5 (all in 0–100 scale; Fig. 1B).

Relationship between LINE-1 methylation levels and chromosomal aberrations

We have previously demonstrated that LINE-1 hypomethylation is associated with a poor prognosis in a study of 217 ESCC paraffin-embedded specimens (23). However, the biologic mechanism by which LINE-1 hypomethylation affects aggressive tumor behavior is not yet fully understood. We hypothesized that global DNA hypomethylation might be a crucial influential factor for DNA copy number variations. Thus, we carried out a CGH array analysis using three LINE-1–hypomethylated tumors (LINE-1 methylation level, 24.4% for case #1; 31.4% for case #2; and 33.5% for case #3) and three LINE-1–hypermethylated tumors (65.3% for case #4; 65.9% for case #5; and 79.2% for case #6). The analyzed cases were selected based on sufficient amount of freshly frozen tissues and sufficient DNA quality. Their clinical and pathologic characteristics are shown in Supplementary Table S1. Pyrograms for cases #1 and #4 are shown in Fig. 1A.

The average number of chromosomal aberrations in 6 ESCC tumors was 168.2 (range, 24–423). Interestingly, LINE-1–hypomethylated tumors showed higher frequency

Published OnlineFirst January 14, 2014; DOI: 10.1158/1078-0432.CCR-13-1645

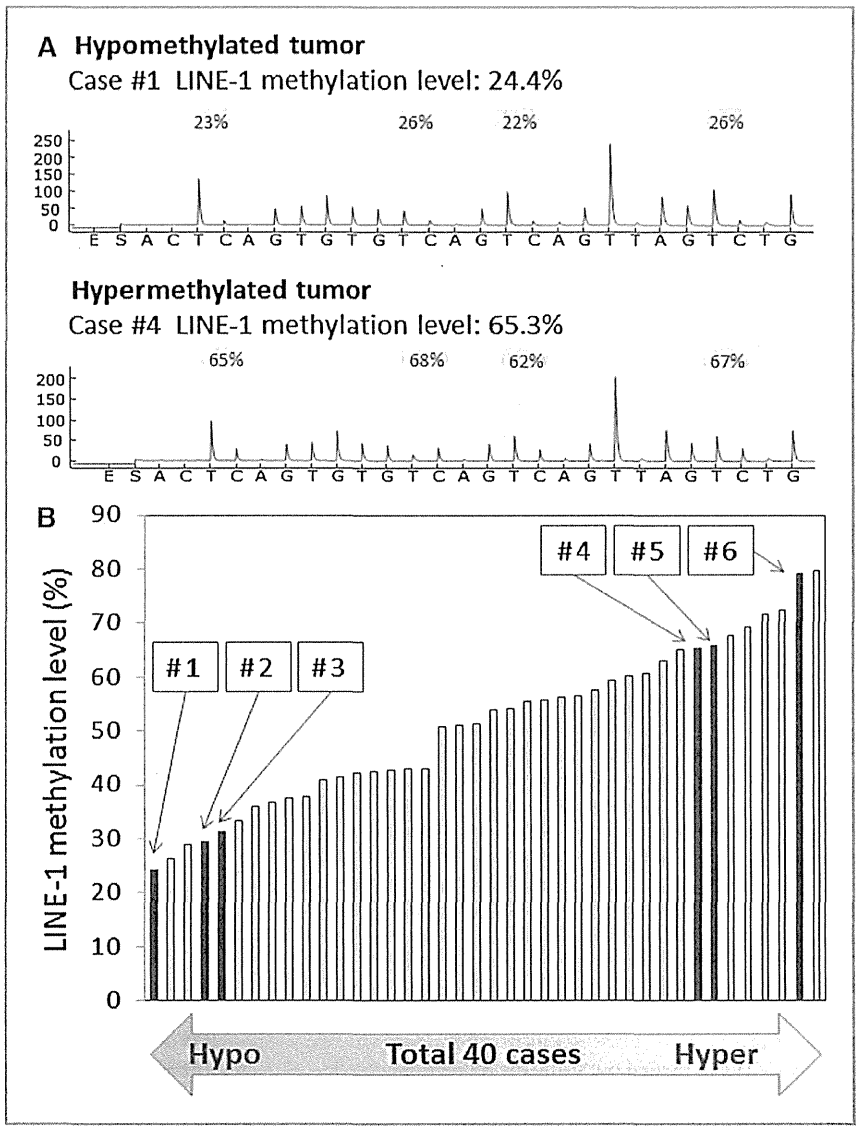

Figure 1. LINE-1 methylation levels in esophageal cancers. A, representative pyrograms for LINE-1 methylation level (cases #1 and #4). B, LINE-1 methylation levels in 40 resected esophageal cancers. Dark stained bars indicate six selected cases for CGH array (#1–3 as LINE-1–hypomethylated cases and #4–6 as LINE-1–hypermethylated cases).

of chromosomal gain or loss compared with LINE-1–hypermethylated tumors. Figure 2A shows a summary of DNA copy number aberrations for LINE-1–hypomethylated tumors and LINE-1–hypermethylated tumors. The number of aberrations was significantly higher in LINE-1–hypomethylated cases (median, 310.0) than in LINE-1–hypermethylated cases (median, 26.3; $P = 0.0076$; Fig. 2B). A similar result was observed for total length of aberrations ($P = 0.0013$; Fig. 2B). Regions with an abnormal number of chromosome copies in all hypomethylated tumors are shown in Table 1. Genomic gains were much more common than losses, and genomic imbalance was not found in chromosome 13, 14, 15, or 16. Amplification of 7q21–22 containing a candidate oncogene *CDK6* was observed in all LINE-1–hypomethylated tumors, whereas this locus was not amplified in all LINE-1–hypermethylated tumors. Previous studies have shown that *CDK6* amplification is associated with CDK6 overexpression and poor survival in esophageal cancer, supporting that CDK6 might mark malignant esophageal cancer (32, 33). From these findings, we further hypothesize that global DNA hypomethylation in ESCC contributes to aggressive phenotype by genomic gain of oncogenes such as *CDK6*. Thus, the correlation between CDK6 aberrant expression (protein and mRNA levels) and LINE-1 hypomethylation in ESCCs was further investigated.

Published OnlineFirst January 14, 2014; DOI: 10.1158/1078-0432.CCR-13-1645

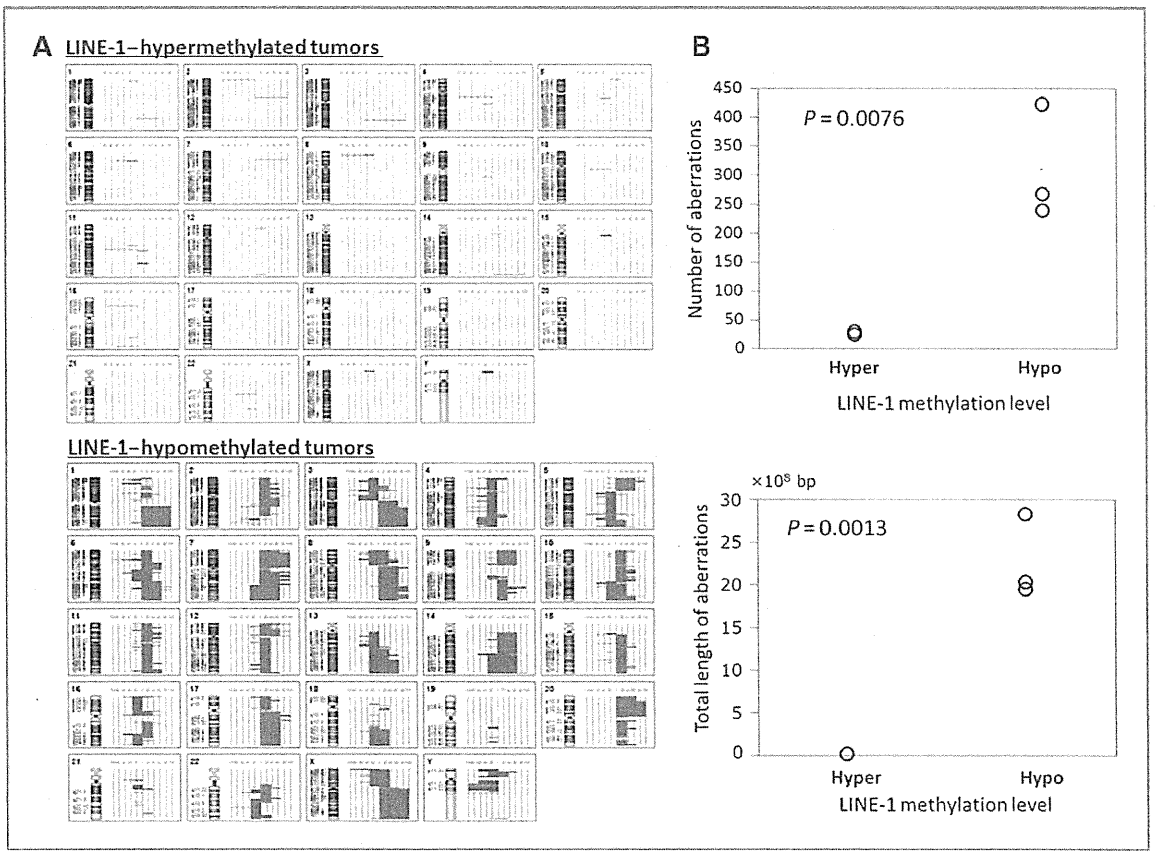

Figure 2. Relationship between chromosomal aberrations and LINE-1 methylation. A, summary of DNA copy number aberrations for LINE-1–hypomethylated cases (top) and LINE-1–hypermethylated cases (bottom). Losses (green) are displayed to the left and gains (red) plotted to the right. B, relationship of LINE-1 methylation status with number of aberrations (top) and total length of aberrations (bottom).

Relationship between CDK6 expression and LINE-1 methylation in ESCC tissues

We measured *CDK6* mRNA expression levels by qRT-PCR in 15 ESCCs tissues and matched normal esophageal mucosa. Cancer tissues showed significantly higher levels of *CDK6* mRNA expression than matched esophageal mucosa ($P = 0.0046$; Fig. 3A). Then, CDK6 expression at the protein level in ESCCs was evaluated by immunohistochemistry. CDK6 immunoreactivity was absent in normal squamous cell epithelium (Fig. 3B-a). Among 40 tumors, 24 tumors (60%) showed CDK6-positive expression (Fig. 3B-b), and 16 tumors (40%) showed CDK6-negative expression (Fig. 3B-c). These observations of CDK6 overexpression may demonstrate that CDK6 has vital roles in ESCC tumorigenesis. To evaluate the impact of LINE-1 hypomethylation on CDK6 expression, we assessed the association between CDK6 expression and LINE-1 methylation levels in ESCC tissues. In 20 ESCCs for which LINE-1 data and RNA were available, *CDK6* mRNA expression levels were inversely associated with LINE-1 methylation levels ($P = 0.039$; Fig. 3C). Tumors with CDK6-positive immunoreactivity exhibited significantly lower LINE-1 methylation levels (median, 42.3; mean, 45.1; SD, 13.1) than tumors with negative immunoreactivity (median, 60.1; mean, 60.0; SD, 12.8; $P = 0.0001$ by the paired t test; Fig. 3D). These results collectively suggest that LINE-1 methylation level (and therefore global DNA methylation level) might have an influence on CDK6 expression through genomic gain of *CDK6*.

Relationship between CDK6 expression and LINE-1 methylation in ESCC cell lines

We then tested this correlation between LINE-1 methylation levels and CDK6 expression levels using nine ESCC cell lines. LINE-1 methylation levels in nine ESCC cell lines were widely distributed (range, 22.8–67.0). The inverse relationship between LINE-1 methylation levels and *CDK6* mRNA expression levels was observed ($P = 0.028$; Fig. 4A). Furthermore, to confirm the gene amplification of *CDK6* in ESCCs, we applied the FISH analysis for TE11 cell line (black dot in Fig. 4B), which demonstrated lower levels of LINE-1 methylation and high levels of *CDK6* mRNA expression *in*

Published OnlineFirst January 14, 2014; DOI: 10.1158/1078-0432.CCR-13-1645

Table 1. Chromosome imbalance regions in LINE-1–hypomethylated tumors

Cytoband	Aberration	Start position	Stop position	Size	Candidate gene	$-\log_{10}(P)$
1q21	Gain	143224322	150145845	6921524	*LOC100130000*	1.30102999
1q21	Gain	150145845	150437139	291295	*ANP32E, CA14*	1.30102999
1q21	Gain	150437139	153949859	3512721		1.30102999
1q21	Gain	153949859	154295703	345845	*JTB, RAB13*	1.30102999
1q21	Gain	154295703	155309112	1013410		1.30102999
1q22	Gain	155309112	155904332	595221	*ASH1L, MIR555*	1.30102999
1q21	Gain	155904332	156796795	892464	*S100A4*	1.30102999
1q21–22	Gain	156815942	161569102	4753161	*NTRK1,INSRR*	1.30102999
1q42	Gain	196800817	225328624	28527808	*CNIH3*	1.30102999
1q42	Gain	225334959	227316832	1981874	*DNAH14,LBR*	1.30102999
1q44	Gain	248738898	248789540	50643	*OR2T10*	1.30102999
1q21	Gain	248789540	249211884	422345	*LOC100130000*	1.30102999
2q21	Gain	50765550	52053468	1287919	*FSHR, NRXN1*	1.30102999
2q35	Loss	219296581	219500621	204041	*VIL1,USP37*	1.30102999
3q21	Loss	50733803	50889948	156146	*DOCK3,p21.2*	1.30102999
3q21	Loss	51474959	51486485	11527	*VPRBP*	1.30102999
3p14	Loss	71118465	71129430	10966	*FOXP1,p13*	1.30102999
3q13	Gain	117950181	162209974	44259794	*IGSF11*	1.30102999
3q29	Gain	193132436	193156879	24444	*ATP13A4,q29*	1.30102999
3q29	Gain	193156879	194964380	1807502	*C3orf21,q29*	1.30102999
4q25	Loss	113504214	113802089	297876	*C4orf21,LARP7*	1.30102999
4q28	Loss	128854114	129114533	260420	*MFSD8*	1.30102999
5p15	Gain	223613	256351	32739	*SDHA, p15.33*	1.30102999
5p15	Gain	822005	887520	65516	*ZDHHC11*	1.30102999
5p15	Gain	9197190	14749366	5552177	*SEMA5A*	1.30102999
5q31	Loss	125891676	125896749	5074	*ALDH7A1*	1.30102999
6p21	Loss	32542694	32565064	22371	*HLA-DRB1*	1.30102999
6q22	Gain	125315619	125934949	619331	*RNF217*	1.30102999
6q23	Gain	134625874	134958897	333024	*SGK1,CpG:21*	1.30102999
7p22	Gain	1886724	2203806	317083	*MAD1L1,CpG*	1.30102999
7p21	Gain	7283309	26893878	19610570	*C1GALT1*	1.30102999
7q31	Gain	26930268	55712859	28782592	*LANCL2*	1.30102999
7q11	Gain	69085548	70537428	1451881	*AUTS2,CpG*	1.30102999
7q21	Gain	78545354	86367244	7821891	*MAGI2*	1.30102999
7q21–22	Gain	92247365	96665717	4418353	*CDK6*	1.30102999
7q31	Gain	107825148	110714112	2888965	*NRCAM*	1.30102999
8q11	Gain	49434350	54585979	5151630	*EFCAB1,SNAI2*	1.30102999
8q21	Gain	75130234	79574535	4444302	*JPH1,GDAP1*	1.30102999
8q22	Gain	105068014	120115974	15047961	*RIMS2,TM7SF4*	1.30102999
8q24	Gain	131275342	140955982	9680641	*ASAP1*	1.30102999
9q21	Gain	82261109	94649728	12388620	*TMC1,TLE4,TLE1*	1.30102999
9q22	Gain	104105604	109937886	5832283	*BAAT, MRPL50*	1.30102999
9q33	Gain	117848315	121937952	4089638	*TNC, DEC1*	1.30102999
10q11	Gain	52685729	63413583	10727855	*PRKG1,MIR605,ZNF488,RBP3*	1.30102999
10q11	Gain	77139109	83286274	6147166	*LOC441666,ZNF503*	1.30102999
10q26	Gain	124348251	124351778	3528	*DMBT1,q26.13*	1.30102999
11p11	Gain	49170280	49714750	544471	*FOLH1*	1.30102999
11q22	Gain	107091691	107502415	410725	*CWF19L2*	1.30102999
12p13	Gain	2690550	2786288	95739	*CACNA1C*	1.30102999
12p12	Gain	21613937	21622974	9038	*PYROXD1*	1.30102999
12p11	Gain	33663998	34591668	927671	*ALG10,CpG:25*	1.30102999

(Continued on the following page)

Published OnlineFirst January 14, 2014; DOI: 10.1158/1078-0432.CCR-13-1645

Table 1. Chromosome imbalance regions in LINE-1–hypomethylated tumors (Cont'd)

Cytoband	Aberration	Start position	Stop position	Size	Candidate gene	$-\log_{10}(P)$
17q11	Gain	31344645	33156978	1812334	*ACCN1,CCL2*	1.30102999
17q21	Gain	39092472	39890632	798161	*KRT23,KRT39*	1.30102999
20p13	Gain	6343032	25493634	19150603	*DEFB125,BMP2,HAO1*	1.30102999
20q12–13	Gain	40674508	41626812	952305	*PLCG1,ZHX3,PTPRT, q12*	1.30102999
20q13	Gain	60895001	62070367	1175367	*BMP7,SPO11,LAMA5,RPS21*	1.30102999
X	Gain	62063537	154788597	92725061	*SPIN4*	1.30102999
Y	Loss	17972056	26066972	8094917		1.30102999
Y	Loss	28548426	28784095	235670	*CpG:32,q11.23*	1.30102999

vitro. We counted the number of signals for *CDK6* and chromosome 7 centromere (control) in 100 TE11 cells. In 91 of 100 cells, the number of signals for *CDK6* was larger than that for chromosome 7 centromere (Supplementary Table S2), confirming the presence of *CDK6* amplification in ESCC cells.

CDK6 expression, LINE-1 hypomethylation, and patient survival

To understand the relationship between CDK6 and tumor malignant behavior in ESCC, we examined the prognostic role of CDK6 in 129 cases with available LINE-1 methylation data and CDK6 expression data. All cases received no preoperative treatment. The relationships between levels of LINE-1 methylation and clinical and pathologic features are summarized in Supplementary Table S3. The median follow-up time for censored patients was 2.7 years. Patients with tumor expressing CDK6 (n = 61) experienced lower disease-free survival rates than patients not expressing CDK6 (n = 68; log-rank P = 0.043, Fig. 5A). This result certainly implies that CDK6 may have oncogenic roles in ESCC and contribute to ESCC progression.

We next examined whether the influence of LINE-1 hypomethylation on patient prognosis was modified by CDK6 expression status. In this current study, LINE-1 hypomethylation was defined as "<55.5" according to our previous article (23). In Kaplan–Meier analysis, patients with LINE-1 hypomethylation (n = 31) experienced significantly shorter disease-free survival compared with LINE-1–hypermethylated cases (n = 98; log-rank P = 0.0005; Fig. 5B). In univariate Cox regression analysis, compared with LINE-1–hypermethylated cases, patients with LINE-1 hypomethylation experienced a significantly higher disease recurrence rate [HR, 2.69; 95% confidence interval (CI), 1.48–4.78; P = 0.0015; Fig. 5C]. In the CDK6-adjusted Cox

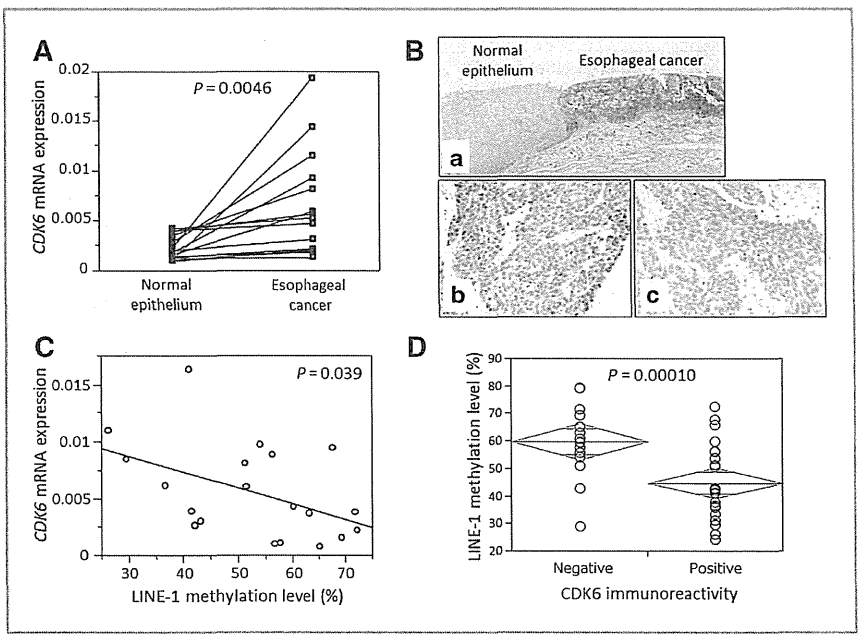

Figure 3. Association of CDK6 expression and LINE-1 methylation levels. A, *CDK6* mRNA expression levels in esophageal cancers and matched normal mucosa. The cancer tissues showed significantly higher levels of expression than the matched normal mucosa (P = 0.0046 by the paired t test). B, a, CDK6 immunostaining for esophageal cancer and normal esophageal mucosa. Cancerous lesion shows positive staining, whereas normal mucosa shows negative staining. b, positive expression of CDK6 in nuclei of esophageal cancer cells. c, negative expression of CDK6 in nuclei of esophageal cancer cells. C, correlation between LINE-1 methylation levels and *CDK6* mRNA expression levels. D, CDK6-positive tumors showed significantly lower levels of LINE-1 methylation than CDK6-negative tumors (P = 0.00010 by the paired t test).

Published OnlineFirst January 14, 2014; DOI: 10.1158/1078-0432.CCR-13-1645

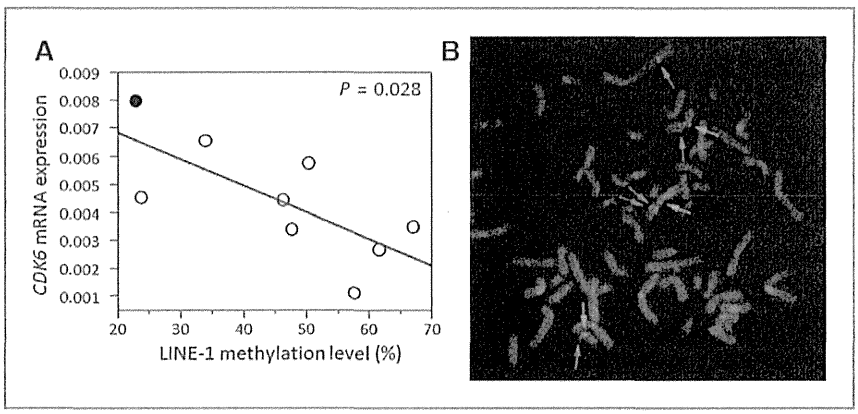

Figure 4. *CDK6* mRNA expression and *CDK6* amplification in ESCC cell lines. A, relationship between LINE-1 methylation levels and *CDK6* mRNA expression levels. Black spots indicate TE11 cell lines analyzed by FISH. B, FISH images with the *CDK6* probe (red) and the chromosome 7 centromere probe (green; control).

model, the HR of LINE-1 hypomethylation for disease recurrence was decreased to 2.25 (95% CI, 1.22–4.04). Thus, this result shows the proportional reduction in the regression coefficient for LINE-1 methylation due to the inclusion of CDK6 expression in the Cox regression model. In the multivariate Cox model adjusted for sex (male vs. female), age at surgery (<64 vs. 65≤), tumor location (upper vs. lower), tumor stage (stage I vs. II, III), histologic grade (G1 vs. G2–4), and CDK6 expression (positive vs. negative), LINE-1 hypomethylation was found to be associated with a significantly higher recurrence rate (multivariate HR, 2.43; 95% CI, 1.19–4.89; $P = 0.016$).

Cyclin D1 expression, LINE-1 methylation level, and patient survival

Given that cyclin D1 is the positive regulatory partner of CDK6, we further examined the relationship between cyclin D1 expression, LINE-1 methylation, and patient outcome. No relationship was observed between cyclin D1 expression and level of LINE-1 methylation ($P = 0.94$; Supplementary Fig. S2A and S2B). We also found no association between status of cyclin D1 expression and disease-free survival (log-rank $P = 0.60$; Supplementary Fig. S2C). Furthermore, the prognostic impact of LINE-1 hypomethylation was not reduced by cyclin D1 expression (cyclin D1-adjusted HR, 2.74; 95% CI, 1.51–4.88).

Discussion

We previously demonstrated the correlation between LINE-1 hypomethylation (i.e., global DNA hypomethylation) and poor prognosis in ESCCs (23). In this current study, to clarify the mechanism by which LINE-1 hypomethylation affects ESCC aggressive behavior, we investigated

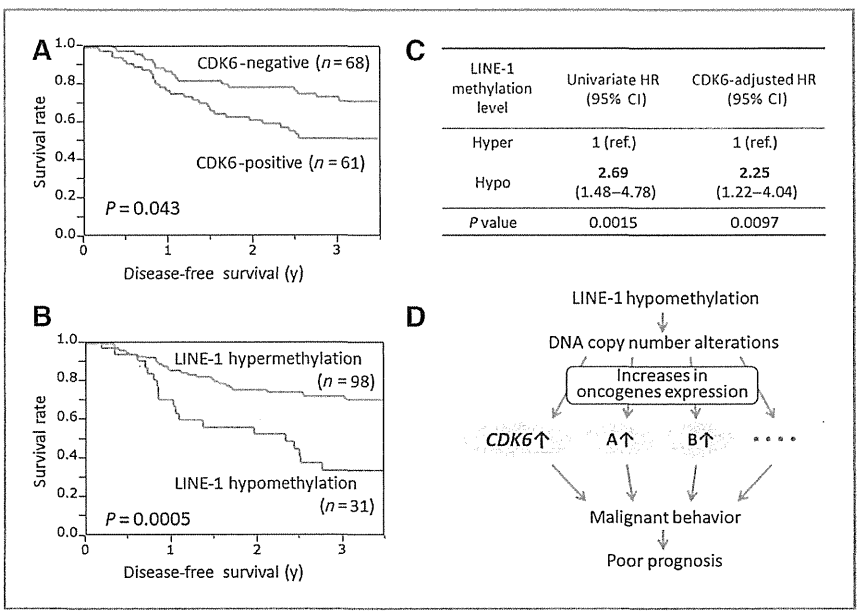

Figure 5. Survival analyses of CDK6 expression and LINE-1 methylation level. A, Kaplan–Meier curves according to CDK6 expression status. B, Kaplan–Meier curves according to LINE-1 methylation status. C, patients with LINE-1 hypomethylation experienced a significantly higher disease recurrence rate (HR, 2.69). In the CDK6-adjusted Cox model, the HR of LINE-1 hypomethylation for disease recurrence was decreased to 2.25. D, possible mechanism by which LINE-1 hypomethylation confers a poor prognosis in ESCC.

Published OnlineFirst January 14, 2014; DOI: 10.1158/1078-0432.CCR-13-1645

LINE-1–hypomethylated and LINE-1–hypermethylated tumors using CGH array. We found that LINE-1–hypomethylated tumors presented highly frequent genomic gains at various loci containing candidate oncogenes including *CDK6*. The association between *CDK6* amplification, CDK6 expression, and LINE-1 methylation levels in ESCCs was also observed. CDK6 expression was significantly associated with unfavorable prognosis in 128 patients with ESCC. Moreover, we have shown the proportional reduction in the regression coefficient for LINE-1 methylation due to the inclusion of CDK6 expression in the Cox regression model. Collectively, CDK6 may be an intermediate factor explaining the relationship between LINE-1 hypomethylation and poor prognosis. Global DNA hypomethylation in ESCC might contribute to the acquisition of tumor aggressive behavior through genomic gains of oncogenes such as *CDK6* (Fig. 5D).

LINE-1 represents a major repetitive element and occupies approximately 17% of the human genome. Thus, the level of LINE-1 methylation is regarded to be a surrogate marker of global DNA methylation (13). Tumor LINE-1 hypomethylation has been associated with inferior prognosis in not only ESCC but also many different human tumor types such as colon cancer, glioma, ovarian cancer, lung cancer, and gastric cancer (17–22). In addition, LINE-1 hypomethylation was associated with clinically aggressive disease in patients with prostate cancer and gastrointestinal stromal tumors (16, 34). Nonetheless, the mechanism by which tumoral LINE-1 hypomethylation correlates with malignant phenotype or patient prognosis in human cancers remains to be fully explored. Experimental evidence supports the relationship between LINE-1 hypomethylation (i.e., global DNA hypomethylation) and genomic instability. A study using $Nf1^{+/-}$ $p53^{+/-}$ mice has shown that introduction of a hypomorphic *Dnmt1* allele causes genome-wide DNA hypomethylation that leads to significant increases in the loss of heterozygosity rate and tumor development (35). Another study has shown that genomic hypomethylation in $Apc^{Min/+}$ mice leads to increases in microadenoma formation through loss of heterozygosity at the *Apc* locus (36). Thus, we carried out an array CGH analysis to assess the potential implication of LINE-1 hypomethylation in genomic instability. Interestingly, LINE-1–hypomethylated tumors showed highly frequent genomic gains at various loci containing numerous candidate oncogenes. Our finding is likely consistent with aforementioned experimental results.

In recent years, high-resolution array-based CGH has been applied to identify target oncogenes and tumor suppressor genes through defining recurrent gains and losses in various cancers (37). Two studies with CGH array analysis for ESCC samples have revealed high-level amplifications at 3q27.1, 7p11, 8q21.11, 8q24.21, 11q13.3, 11q22, 12q15–q21.1, 18q11.2, and 19q13.11–q13.12, and homozygous deletions at 4q34.3–q35.1 and 9p21.3 (38, 39). Bandla and colleagues conducted a comprehensive analysis of DNA copy number abnormalities in both ESCCs and esophageal adenocarcinoma. They reported a number of oncogenes that were amplified in both histologic types, including *CDK6*, *MCL1*, *EGFR*, *SMURF1*, *KRAS*, *ERBB2*, *CCNE1*, *VEGFA*, *MET*, and *IGF1R* (32). Among these genes, *CDK6* amplification has been associated with CDK6 overexpression and a poor survival in esophageal cancer (33), supporting that CDK6 might mark esophageal cancer with aggressive biologic behavior. We also found that CDK6 expression was related with a poor prognosis in ESCCs. These results certainly imply that CDK6 has oncogenic roles in ESCC and contributes to ESCC progression. Our finding of the correlation between LINE-1 hypomethylation, *CDK6* amplification, and CDK6 aberrant expression suggests that LINE-1–hypomethylated tumors might acquire malignant aggressive behavior by increasing genomic amplification and by altering the expression levels of candidate oncogenes represented by *CDK6*. However, other mechanisms may also be involved. In addition to its role as a surrogate marker for global DNA methylation, LINE-1 methylation status by itself likely has biologic effects, because retrotransposons such as LINE-1 elements can provide alternative promoters and contribute to noncoding RNA expression, which regulates the functions of a number of genes.

CDK6, which belongs to a family of serine–threonine kinases, is an important regulator of G_1–S-phase progression. Together with its binding partner cyclin D1, CDK6 forms active complexes that promote cellular proliferation by phosphorylating and inactivating the retinoblastoma protein (40). *CDK6* amplification has been previously reported in human neoplasms including esophageal cancer, in which (in most cases) it is correlated with an adverse prognosis (33). Our current study revealed a relationship between CDK6 expression and LINE-1 hypomethylation (i.e., global DNA hypomethylation) and poor prognosis, suggesting that aberrant expression of CDK6 might be epigenetically regulated, and mark an aggressive type of esophageal cancer. Importantly, the current study found no relationship between cyclin D1 expression and LINE-1 hypomethylation, suggesting that, with regard to G_1/transition regulation, cyclin D1 is regulated by an entirely different mechanism from that of CDK6.

Interestingly, CDK6 is capable of blocking cell differentiation apart from the classical role in promoting cell proliferation (41, 42). This uniqueness makes it an attractive candidate for the development of small-molecule inhibitors. PD-0332991 is a recently developed specific inhibitor targeting CDK4/6-specific phosphorylation of retinoblastoma protein, and is currently in phase I clinical trials for advanced cancers (43). This small-molecule inhibitor has been shown to potently suppress proliferation and anchorage-independent growth of esophageal cancer cell lines (33). Hereafter, CDK6 expression in the resected specimens might attract increasing attention as a biomarker for patient selection. In this respect, our findings may have clinical implications.